

RFID Integration with Internet of Things: Data Processing Algorithm Based on Convolutional Neural Network

Liang Wang*

School of Electrical Engineering, Hunan Mechanical & Electrical Polytechnic, Changsha, Hunan 410151, China

Abstract—Radio Frequency Identification is a fast and reliable communication module that performs automatic data capture to identify and track individual objects and people. Frequency-coded tags employ resonant networks to decode their unique code. A multi-scatterer or multi-resonant method encodes the data. Research primarily related to the current investigation predicted that the chipless RFID tag resonant network has a high bit encoding capacity. This study addresses the simulation, optimization, fabrication, testing, and data encoding methods for chipless RFID tags. This research provides a framework for the open-ended quarter-wavelength stub multi-resonator method in chipless Radio Frequency Identification (RFID) tags. The proposed design enhances the tag's data encoding capacity and improves its robustness to ecological differences. This study integrates Error Correction Coding (ECC) and Adaptive Modulation Systems (AMS) employing Convolutional Neural Networks (CNN) to enhance the tag's performance. The AMS dynamically alters the modulation parameters based on channel states, while ECC improves data reliability. The results indicate efficient performance compared to traditional chipless RFID tags, highlighting the possibility of practical behavior in typical applications that necessitate reliable and high-capacity data transmission.

Keywords—RFID; chipless; coding; threshold; data transmission; error correction; security authentication

I. INTRODUCTION

Radio Frequency Identification is referred to as RFID. An RFID comprises a reader and one or more tags or transponders. RFID is a new technology. The British radar system employed RFID for the first time in World War II to differentiate between German aircraft and their aircraft that had radio transponders attached. Several industries have benefited from the advantages of RFID, including the military, healthcare, security, sports, animal husbandry, and aviation. RFID has several essential sector-specific applications. RFID is utilized in various applications, including supply chain management, automated payment systems, vehicle tracking, inventory management, secure shop checkouts, animal monitoring, and sports timing technology. RFID transfers data from an electronic tag, frequently known as a label or an RFID tag, using radio waves. Selecting an RFID tag is required. There are numerous frequencies of RFID tags available on the market. Microwave, High Frequency, Low Frequency, and Ultra High Frequency are all included [1-5].

Organizations can now afford to use RFID due to technological advancements in cost factors. Wal-Mart was one of the first industries to use RFID technology for theft prevention and inventory supply process improvements. Wal-Mart mandated that its top 100 suppliers apply RFID tags to the pallets and cases they sent to the company by the end of 2004, marking the start of deploying RFID across its retail distribution chain. However, in 2004, RFID tag producers were unable to meet the demand level within Wal-Mart's targeted timeframe due to the state of standards and limited tag manufacturing capabilities.

With most of their leading suppliers supplying RFID-tagged pallets and crates to every Wal-Mart distribution facility, Wal-Mart's adoption is now well underway as standards change, manufacturing capabilities increase, and price points decline. Although RFID is beginning to infiltrate other business supply chains, these implementations are frequently closed-loop. To put it another way, RFID is implemented within the supply chain of a particular company but not between them and their commercial trade partners. Other applications, including tracking equipment to ensure that it is not left behind in the aircraft after repair, can only be used within a single business [6-10].

Information is stored on transponder tags in all RFID systems. RFID tags hold data that may be as vast as an array of bits or as little as a single binary bit that indicates an identifying code, Aadhaar number, personal medical data, or anything else that can be recorded in digital binary format. Microchips power RFID tags. RFID tags within a specific range may get sufficient power from the field. It transmits the data it has saved and accesses its internal memory using this power [3-4]. The transceiver antenna's voltage increases due to the interaction between the RF fields when the Transponder Tag draws power in this manner. The purpose of the Tag is to convey data to the reader by using this sort of impact. The Tag regulates how much energy is reserved from the field. The Tag controls the voltage detected at the transceiver following the bit pattern it wants to send [11-15].

RFID is an automated data collection that recognizes and monitors individual objects and people in real-time using RFID signals [16-20]. It is used as a radio technology to realize the Internet of Things (IoT) vision of generating a universal system of smart objects [21-26]. It would be possible to mark and invent all items fitted with radio tags. RFID tags must be data-rich, low-cost, and energy-efficient to perform these functions.

*Corresponding Author

The RFID idea was introduced during World War II to find enemy aircraft [27-30].

To distinguish between friend and foe, the radar transmitter receives a backscattered signal from a receiver tagged in an airplane [31-32]. Later, in 1945, Leon Theremin made an intriguing discovery of RFID using the backscattering principle. As a result of the development of RFID, the commercial potential for tracking and identifying objects without physical intervention has increased. Furthermore, RFID can handle a greater number of items than barcodes [33-36]. RFID's main advantages are flexibility and versatility, and it promises to be a future technology in automatic designation [37-40].

RFID and bar code technologies are highly similar, but instead of using a laser to read barcodes on labels, radio frequency waves are used to read information from tags [41-45]. Due to its wide range of applications in various areas, including supply chain management, healthcare, traffic management, commerce, access control, purchasing, and distribution logistics, as well as manufacturing and service industries, substantial research has been conducted in the area of RFID in recent years [46-50]. The RFID tag stores a distinct identification number parallel to a bar code or magnetic strip on the back of a credit card or ATM card. The classification must be processed close to its scanning device to retrieve bar code or magnetic strip data. However, because of the high cost of the silicon chip required, its general application is limited. As a result, low-cost alternatives are in high demand. RFID tags without silicon chips are now being created. These tags are called 'chipless' tags [51-55].

A. Motivation

This research aims to develop a robust and inexpensive sensor network that can integrate various types of sensors, including electrical, chemical, and biological sensors. Wireless sensor tags have historically been used in other settings as active or semi-passive tags for collecting wireless data. A tag's application area is limited by its need for a battery, which reduces its lifespan and increases its cost. Many academics studying passive chipless sensor tags in recent years have been interested in passive RFID sensor tags due to the challenges they face in their development. This study develops two chipless sensor tag designs and a transmission line reflection-based ID generation system, which proposes a wide range of sensor types for evaluation, including nanoparticle-based sensors, microstrip antennas on a flexible substrate, and previously reported transmission delay line-based ID generation schemes. Dipole-based antennas are a standard and attractive option for passive tag designers from a business standpoint; however, their primary drawback is their length. Long straight dipole antennas are miniaturized using folding and meandering methods instead of long straight dipole arms. A tiny tag with excellent reading ranges and comprehensive band behavior is the product of these innovations. Future work aims to further improve the quality, efficiency, and applicability of the sensor tag system developed through this research.

1) *Problem statement and research objective.* A chipped RFID tag is composed of integrated circuits that store the identifying codes. The price of this tag is higher due to the use

of silicon chips. An alternative solution to this difficulty is to develop a chipless RFID tag, which does not contain a silicon chip. The primary challenge in developing a chipless RFID tag is determining how to encode data without a memory chip, which has limited capacity. Multi-resonator-based tags are the combination of multiple resonator circuits and transcoding antenna structures. These antenna networks are called microstrip antennas. The efficient realization of the multi-resonator structure can be built using these microstrip antennas. However, the inherent drawbacks of these microstrip antennas are low gain and narrow bandwidth. The polarization antennas are utilized to address the drawback, and the significant segment is chipless RFID tags, which are retransmission-based multi-resonator tags. The network is designed to address the problems associated with the prominent recognition of chipless RFID tags.

The study on the chipless RFID is written as follows: the overview of RFID, chipless RFID, motivation, and problem statement with research objective are detailed in Section I. The literature review is discussed with a research gap in Section II. The proposed CNN-based coding system is given in Section III, the simulation result is presented with detailed discussion in Section IV, and the study ends with a justified conclusion in Section V.

II. RELATED WORKS

This section explains various studies on chipless RFID. These investigations explore various features, including novel encoding methods, Machine Learning (ML) integration, and system reliability enhancements (see Table I). In [5-6-60], the authors introduce a unique encoding for RFID tags, addressing data capacity limitations. In [61], the authors view the proposals' insights into ML's role in chipless RFID, highlighting challenges and proposing standardized data protocols. In [62], the authors employ ML and DL for robust data reading in CRFID sensor tags. In [63], the authors present a workflow for ML classification in chipless RFID tag identification. In [64], the authors introduce a multi-tag detection system using 1D-CNN. In [65], the authors investigate Deep Learning (DL) to improve RFID tag detection accuracy. In [66], the authors evaluate ML models for identifying information in chipless RFID tags. In [67], the authors propose a phase coding-based RFID tag design, while [68] examines chipless RFID for material identification. In study [69], data-driven methods are suggested to improve chipless RFID reliability.

The research gap identified in the review is the limited resolution of multi-tag detection systems [70]. Conventional frequency-based systems face limitations in achieving high-resolution multi-tag detection, thereby limiting their practical applicability. The application of CNN overcomes these challenges by improving reliability and accuracy in multi-tag detection. CNN leverages advanced pattern recognition capabilities to analyze complex data sets, enabling more precise and efficient tag detection even in challenging environments. This development represents a significant leap forward in chipless RFID technology, addressing the critical research gap

of achieving high-resolution multi-tag detection for practical deployment in numerous applications.

TABLE I SUMMARY OF ML-BASED RFID

Inference	Methods used	Outcome	Drawback
Proposes a novel encoding for chipless RFID tags using N resonant elements with M individual desired frequencies, thereby overcoming the data encoding capacity limitation. PSO algorithm optimizes tag structure parameters.	Particle Swarm Optimization (PSO) algorithm	Overcomes data encoding capacity limitations, enabling the determination of resonant frequencies before the tag model.	Requires optimization for specific tag designs.
Provides a comprehensive review of ML in CRFID technology, highlighting integration challenges and suggesting standardized data protocols for improved ML deployment.	Review of ML approaches, identification of challenges, proposal for standardized data protocols	Identifies challenges in ML integration with CRFID and suggests standardizing data protocols for improved deployment.	The lack of standardized data protocols may hinder ML deployment.
Introduces ML and DL regression modelling for robust CRFID sensor tag data reading—automated data acquisition training on large-scale datasets. 1-D CNN outperforms conventional ML models.	ML and DL regression modelling.	Achieves high accuracy in ID and sensing data detection and outperforms conventional ML models.	Restricted resolution of 3 cm for multi-tag detection.
Presents workflow for ML classification in chipless RFID tag identification, achieving perfect accuracy for four tags under fixed and flexible ranges.	ML classification workflow, optimization of tag responses	Achieves perfect accuracy for tag identification under various ranges and enhances tag responses.	Limited to four tag identifications.
Introduces chipless RFID multi-tag detection system using 1D CNN, achieving 100 per cent accurate multi-tag detection.	1D CNN for multi-tag detection, analysis of CNRs and natural frequencies	Achieves 100 per cent accurate multi-tag detection, outperforming frequency-based systems.	Restricted resolution of 3 cm for multi-tag detection.
Investigates DL techniques to improve chipless RFID tag detection accuracy, achieving roughly 99.99 per cent accuracy.	Evaluation of DL techniques	Achieves significant improvement in detection accuracy, reaching near-perfect accuracy.	Limited discussion on practical implementation challenges.
Evaluate ML models for detecting identification and sensing information in RCS-based chipless RFID tags, achieving high accuracy with SVR and GBT models.	Evaluation of ML	Achieves high accuracy in identification and sensing data detection.	Lack of discussion on real-world applicability.
Proposes a phase coding-based chipless RFID tag design featuring a C-shaped resonator capable of achieving 243 distinct states.	Proposal of phase coding-based chipless RFID tag design	Achieves high coding capacity with smaller tag dimensions.	Limited experimental validation was provided.
Examines the utility of chipless RFID technology for material identification, achieving over 90 per cent accuracy and faster detection speed compared to literature methods.	Examination of chipless RFID technology for material identification	Achieves high accuracy and faster detection speed, demonstrating practical utility.	May sacrifice accuracy for improved detection speed.
Proposes data-driven methods to enhance chip-less RFID interrogation and reliability, achieving high validation accuracy and increased reading range.	Proposal of data-driven methods, analysis of chip-less RFID tags	Achieves high validation accuracy and increased reading range, enhancing system reliability	It may require further optimization for specific environments.

III. PROPOSED CHIPLESS RFID TAGS IN ADAPTIVE MODULATION AND ERROR CORRECTION CODING USING CNN

This section deals with the design and development of retransmission-based resonating structures and encoding of the resonating structures. The three key elements of the retransmission-based tags are the transmitting (T_x) and receiving (R_x) antennas, as well as multi-resonating structures. The multi-resonator network plays a vital part in frequency-coded tags. It is a combination of multiple narrow-band rejection filtering sections, each comprising several resonators, used to encode the tag identity. These resonating structures will

alter the interrogating signal's amplitude. The filter's performance is coupled to a transmission line, which sends the encrypted signal data to the reader.

The multi-resonator-based tags are proposed on microstrip-based planar resonators, which are either coupled or connected to the transmission line. The different networks of multi-resonators are presented in this section. The designed multi-resonating structures depends on the operating frequency band, the separation between the resonators, and the properties of the substrate. The multi-resonator consists of multiple resonators in the microstrip line, and each resonator resonates at its quarter wavelength frequency. The designed multi-resonators are

simulated on a low-cost FR4 substrate with a dielectric constant of 4.4, a loss tangent of 0.0018, and a height of 1.6 mm using an Advanced Design System (ADS). The bottom plane acts as a ground plane [71-76].

Open-ended quarter-wavelength stub multi-resonators are designed to overcome the size limitation of the above "L" shaped arm multi-resonator. To solve the constraints of short stub multi-resonators, several open stub multi-resonators have been proposed. A simple, open-ended quarter-wavelength multi-resonator is proposed. As a result, the tag size will be reduced by 50 per cent. The ten stubs are connected to a 50-ohm impedance microstrip transmission line in the multi-resonator. The microstrip transmission line width (3 mm), as in Eq. (1) and Eq. (2):

$$\frac{W}{h} = \begin{cases} \frac{8e^A}{e^{2A}-2} & \text{for } \frac{W}{h} < 2 \\ \frac{2}{\pi} \left[B - 1 - \ln(2B - 1) + \frac{\epsilon_r - 1}{2\epsilon_r} \left\{ \ln(B - 1) + 0.39 - \frac{0.61}{\epsilon_r} \right\} \right] & \text{for } \frac{W}{h} \geq 2 \end{cases} \quad (1)$$

where,

$$A = \frac{z_0}{60} \sqrt{\frac{\epsilon_r + 1}{2}} + \frac{\epsilon_r - 1}{\epsilon_r + 1} \left(0.23 + \frac{0.11}{\epsilon_r} \right) \text{ and } B = \frac{377\pi}{2z_0\sqrt{\epsilon_r}} \quad (2)$$

The length (17 mm) of the microstrip transmission line by Eq. (3) and Eq. (4):

$$\phi = 90^\circ = \beta L_f = \sqrt{\epsilon_{eff}} K_0 L_f \quad (3)$$

$$L_f = \frac{90^\circ \left(\frac{\pi}{180^\circ} \right)}{\sqrt{\epsilon_{eff}} K_0} \quad (4)$$

where,

- $K_0 \rightarrow$ The phase constant and is equal to $2\pi/\lambda$.

The open-ended quarter-wavelength resonator behaves as a series RLC resonant circuit. So, each resonator is modelled as a quarter wavelength.

The input impedance of a lossy transmission line is given in Eq. (5):

$$Z_{in} = Z_0 \frac{Z_L + Z_0 \tanh \gamma l}{Z_0 + Z_L \tanh \gamma l} \quad (5)$$

where, $\gamma = \alpha + j\beta$

For an open-circuited lossy transmission line, the input impedance is given in Eq. (6) and Eq. (7):

$$Z_{in} = Z_0 \coth(\alpha + j\beta) l \quad (6)$$

$$Z_{in} = Z_0 \frac{1 + j \tan \beta l \tanh \alpha l}{\tanh \alpha l + j \tan \beta l} \quad (7)$$

In real-time applications, the transmission line has a slight loss, so $\alpha l \ll 1$ and $\tanh \alpha l \approx \alpha l$

Assume

$$\omega = \omega_o + \Delta\omega \quad (8)$$

where, is $\Delta\omega$ Small [see Eq. (8) and Eq. (9)].

$$\beta l = \frac{\omega l}{v_p} = \frac{\omega_o l}{v_p} + \frac{\Delta\omega l}{v_p} = \frac{\pi}{2} + \frac{\pi\Delta\omega}{2\omega_o} \quad (9)$$

Then

$$\cot \beta l = \cot \left(\frac{\pi}{2} + \frac{\pi\Delta\omega}{2\omega_o} \right) = -\tan \left(\frac{\pi\Delta\omega}{2\omega_o} \right) = \frac{\pi\Delta\omega}{2\omega_o} \quad (10)$$

as in Eq. (10). From Eq. (11),

$$Z_{in} \approx Z_o \frac{1 + j\alpha l \frac{\pi\Delta\omega}{2\omega_o}}{\alpha l + j \frac{\pi\Delta\omega}{2\omega_o}} \approx Z_o \left[\frac{1}{\alpha l} + j \frac{\pi\Delta\omega}{2\omega_o} \right] \quad (11)$$

It indicates the input impedance of a series RLC resonant circuit. The quality factor is given in Eq. (12):

$$Q = \frac{L\omega_o}{R} = \frac{\pi}{4\alpha l} \approx \frac{\beta}{2\alpha} \quad (12)$$

The proposed design has to generate resonance by optimizing the length of an open-ended stub resonator. Each resonator length is computed as in Eq. (13):

$$W_t = \frac{\lambda g}{4} \quad (13)$$

where,

- $W_t \rightarrow$ The open stub resonator length at 2.08 GHz resonant frequency
- The open-ended stub resonator length is approximately 20.8 mm.

Other stub lengths are computed using the same procedure and the values (see Table II). The proposed multi-resonating structure is implemented on an FR4 substrate with a dielectric constant of 4.4 and a loss tangent of 0.0018. The conductor thickness is 35 μm . The mutual coupling of open stub resonators is reduced when the stubs are held 1 mm apart. The bottom plane serves as a ground plane. The span of the proposed design is 23.8 mm \times 17 mm.

TABLE II LENGTH OF THE 10-BIT OPEN STUBS

Stubs	Resonant Frequency (GHz)	Length of the open stubs (mm)
1	2.08	20.8
2	2.22	18.5
3	2.36	17.4
4	2.59	15.8
5	2.80	14.5
6	2.96	13.7
7	3.19	12.5
8	3.41	11.5
9	3.68	11
10	3.84	10.4

As the open stub microstrip line resonator resonates at the desired frequency, the wavelength remains $1/4$ of its original wavelength ($\lambda/4$). Because of its inductive solid reactance, the resonator has a good quality factor, which prevents nearby resonant frequencies from merging. It is an actual electric current induced by an applied electromagnetic field. It shows the maximum current at the resonant frequency of 2.08 GHz. For efficient chipless RFID tag realization, the space limitation of open-stub multi-resonators can be replaced by meandered-line multi-resonators. The procedure of chipless RFID design is given in Algorithm 1.

Algorithm 1. Muti-Resonator Based Chipless RFID Design

1. *DefineKeyConstituents()*:
 - Define Tx and Rx antennas.
 - Define multi-resonating structures.
 2. *DesignMultiResonatorStructure()*:
 - Combine multiple narrow-band rejection filtering sections using several resonators.
 - Simulate the designed multi-resonators on a substrate.
 3. *DesignOpenEndedStubs()*:
 - Design open-ended quarter-wavelength stub multi-resonators.
 - Calculate the dimensions of the microstrip transmission line.
 4. *ModelResonators()*:
 - Model each resonator as a quarter wavelength to behave as a series RLC resonant circuit.
 - Determine the input impedance of the lossy transmission line.
 5. *OptimizeResonatorLengths()*:
 - Optimize the length of each open-ended stub resonator to generate resonance.
 - Calculate resonator lengths.
 6. *ImplementMultiResonatingStructure()*:
 - Implement the proposed multi-resonating structure on the substrate.
 7. *VerifyResonantBehavior()*:
 - Verify the resonators' resonant behaviour and quality factor at desired frequencies.
 8. *ConsiderAlternativeDesigns()*:
 - Consider alternative designs such as meandered line multi-resonators if necessary.
- Main()*:
- *DefineKeyConstituents()*
 - *DesignMultiResonatorStructure()*
 - *DesignOpenEndedStubs()*
 - *ModelResonators()*
 - *OptimizeResonatorLengths()*
 - *ImplementMultiResonatingStructure()*
 - *VerifyResonantBehavior()*
 - *ConsiderAlternativeDesigns()*
-

Collect data from chipless RFID tags, including the response patterns generated by multi-resonator networks. Encode the collected data into a format suitable for training the CNN. This encoding may involve mapping the RFID tag responses to specific modulation and coding methods. The signal response is modelled using Eq. (14):

$$y(t) = \sum_{n=1}^N A_n \cdot \sin(2\pi f_n t + \phi_n) \quad (14)$$

The adaptive amplitude and phase modulation are given in Eq. (15) and Eq. (16).

$$A_n = f(A_{n-1}, \theta_n) \quad (15)$$

$$\phi_n = f(\phi_{n-1}, \theta_n) \quad (16)$$

Eq. (14) is the signal response modelling of a chipless RFID tag. The received signal 'y(t)' is expressed as a summation of sinusoidal components, where each component 'n' is characterized by its amplitude 'A_n', frequency 'f_n', and phase

'φ_n'. It captures the fundamental behavior of the tag's response to an interrogating signal.

The FE from the multi-resonator RFID signal, Eq. (17):

$$X = [x_1, x_2, x_3, \dots, x_n] \quad (17)$$

In Feature Extraction (FE) [Eq. (17)], the extracted features from the RFID signal are represented as a vector $X = [x_1, x_2, x_3, \dots, x_n]$. To provide the signal's encoding in a feature space compatible with the next processing step, each x_i represents a distinct FE from the RFID data.

The convolutional layer is a key component of coding for multi-resonator chipless RFID tags, as it analyses the data signal input sent from the tags. The Neural Network (NN) can extract valuable features and patterns from the RFID tag data due to the convolution techniques applied to the input data in this layer. The convolution layer utilizes filter learning to train the neural network (NN) to detect specific frequency resonances and store them in a format suitable for future investigation. To integrate non-linearities into the NN, an activation function is used following the convolutional layer. The system's ability to detect minor variations in the RFID signal is boosted by this non-linearity, allowing it to identify significant variations and connections within the resonator responses. The features are transmitted forward to the Fully Connected (FC) layer, which is then extracted and analyzed by the convolutional layers, where they are flattened. To ensure a deep examination and summary of the extracted features, all neurons in this layer are connected to all the neurons in the layer before it. Here, researchers enhance the input signal description by adjusting weights and biases, enabling the provision of an accurate output prediction. The proper recognition and decoding of data encoded within the chipless RFID system are rendered possible by the valuable information obtained through the resultant prediction from the FC layer about the features and IDs of the RFID tags. From Eq. (18) to Eq. (22), this study tests CNN.

$$Z^{[1]} = W^{[1]} \times X + b^{[1]} \quad (18)$$

$$A^{[1]} = g(Z^{[1]}) \quad (19)$$

$$Z^{[2]} = W^{[2]} A^{[1]} + b^{[2]} \quad (20)$$

$$A^{[2]} = g(Z^{[2]}) \quad (21)$$

$$\hat{Y} = A^{[2]} \quad (22)$$

Eq. (18) to Eq. (22) describe the operations within a CNN. Eq. (18) calculates the activation of neurons in the convolutional layer by convolving the input data 'X' with learnable filters $W^{[1]}$ and adding a bias term $b^{[1]}$. The activation is then passed using an activation function g [Eq. (6)]. In Eq. (7), the FC layer computes the activation using weights $W^{[1]}$ and bias term $b^{[2]}$. The activation is again passed through an activation function in Eq. (22).

$$C = E \times G \quad (23)$$

$$\hat{E} = f(Y) \quad (24)$$

$$d = \text{dist}(Y, \hat{Y}) \quad (25)$$

Eq. (23) to Eq. (25) pertain to ECC. Eq. (23) involves generating a codeword ‘C’ from an information vector ‘E’ by multiplying it with a generator matrix G. Eq. (24) performs error correction by applying a function ‘f’ to the received vector ‘Y’ to predict the data vector ‘E-hat’. The Hamming distance ‘d’ between the received and computed vectors is computed in Eq. (25). Adaptive modulation is given in Eq. (26) to Eq. (28).

$$P_{out} = P_{in} \times \eta \quad (26)$$

$$BER = f(P_{out}, SNR) \quad (27)$$

$$ModScheme = g(BER) \quad (28)$$

Adaptive modulation in chipless RFID adjusts power (P_{out}) via efficiency factor η , calculates Bit Error Rate (BER) from P_{out} and SNR, and selects modulation scheme based on BER $ModScheme$. It optimizes power usage and modulation for reliable communication in dynamic RFID. The procedure for error correction using a CNN is outlined in Algorithm 2.

Algorithm 2: ECC Scheme using CNN

1. Collect data from chipless RFID tags, including response patterns from multi-resonator structures.
2. Encode collected data into a format suitable for training the CNN model.
3. Define signal response modeling function: $\mathbf{y}(\mathbf{t}) = \sum_{n=1}^N \mathbf{A}_n \cdot \sin(2\pi \mathbf{f}_n \mathbf{t} + \phi_n)$
4. Extract features from the RFID signal: $\mathbf{X} = [\mathbf{x}_1, \mathbf{x}_2, \mathbf{x}_3, \dots, \dots, \mathbf{x}_n]$
5. Define convolutional layer operations: $\mathbf{Z}^{[1]} = \mathbf{W}^{[1]} \times \mathbf{X} + \mathbf{b}^{[1]}$
 $\mathbf{A}^{[1]} = g(\mathbf{Z}^{[1]})$
6. Define FC layer operations: $\mathbf{Z}^{[2]} = \mathbf{W}^{[2]} \mathbf{A}^{[1]} + \mathbf{b}^{[2]}$
 $\mathbf{A}^{[2]} = g(\mathbf{Z}^{[2]})$
7. Obtain output prediction: $\hat{\mathbf{Y}} = \mathbf{A}^{[2]}$
8. Define ECC operations:
 $\mathbf{C} = \mathbf{E} \times \mathbf{G}$
 $\hat{\mathbf{E}} = f(\mathbf{Y})$
 $\mathbf{d} = \text{dist}(\mathbf{Y}, \hat{\mathbf{Y}})$
9. Define adaptive modulation operations:
 $P_{out} = P_{in} \times \eta$
 $BER = f(P_{out}, SNR)$
 $ModScheme = g(BER)$

IV. RESULTS AND DISCUSSION

By employing PyTorch, developers can build a CNN by describing layers, activation functions, and additional features that enables you to set up the error correction coding algorithm. For effective data handling, use PyTorch’s Dataset and DataLoader classes. Use a dataset that includes behaviour patterns from multi-resonator chipless RFID tags. Select an appropriate optimization algorithm (Adam) and loss function (CrossEntropyLoss) and set up a training loop to evaluate the dataset, compute gradients, and adjust model parameters. Model performance can be optimized by adjusting hyperparameters such as learning rate and batch size. To set up error correction coding in multi-resonator chipless RFID tags, follow these steps and utilize PyTorch’s features to develop and train a Convolutional Neural Network (CNN). Eq. (29) to Eq.

(33) are employed to assess the performance of the CNN-based ECC.

$$SNR = \frac{Signal\ Power}{Noise\ Power} \quad (29)$$

$$BER = \frac{Number\ of\ Bit\ Errors}{Sum\ of\ Bits} \quad (30)$$

$$SER = \frac{Number\ of\ Symbol\ Errors}{Sum\ of\ Symbols} \quad (31)$$

$$FER = \frac{Number\ of\ Frame\ Errors}{Sum\ of\ Frames} \quad (32)$$

$$Capacity = \frac{Data\ Rate}{bandwidth} \quad (33)$$

Key metrics of communication network performance are presented by Eq. (30) to Eq. (33). Eq. (29) defines the Signal-to-Noise Ratio (SNR) as a basic measurement used to measure signal quality since it measures the ratio of signal power to noise power. BER, which is an essential statistic for measuring transmission accuracy, is computed by Eq. (30). BER is the ratio of error bits to all bits received. Eq. (31) can be employed to derive the Symbol Error Rate (SER), which measures the accuracy of symbols at the symbol level. It is the ratio of wrong received symbols to the complete transmitted symbols. Frame Error Rate (FER) is a vital factor in assessing data packet integrity; it is computed by Eq. (32) and is described as the ratio of wrongly received bytes to the number of transmitted bytes. As the final step in determining manipulative channel efficiency, Eq. (33) computes size, which represents the highest possible data rate that can be achieved with a particular frequency (see Table III). The optimization and evaluation of communication system efficacy in various scenarios rely on these metrics.

TABLE III COMPARISON OF PERFORMANCE

Performance Measures (bits)	PSO	1D-CNN	MR-CNN
SNR	454.78	678.67	767.78
BER	567.23	432.13	232.13
SER	678.56	612.67	412.78
FER	567.56	512.68	354.78
Capacity	31.23	45.4	53

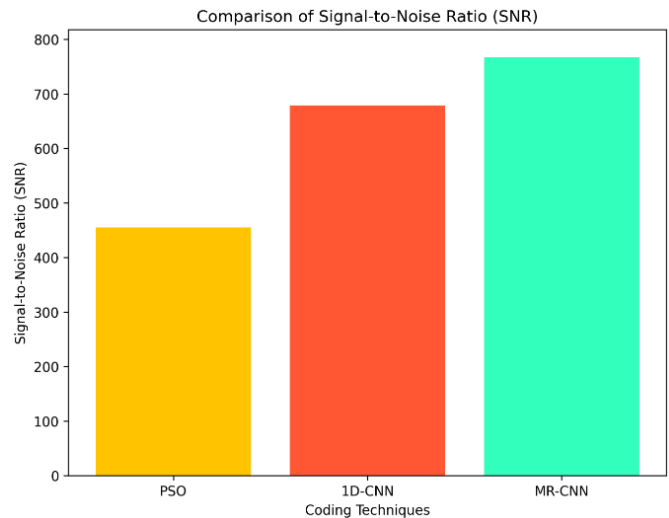


Fig. 1. Comparison of SNR

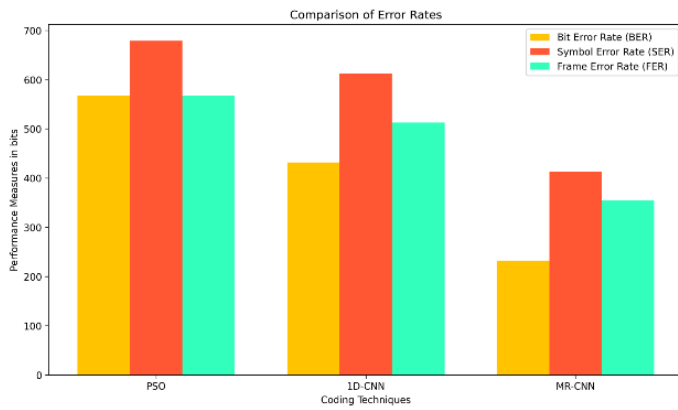


Fig. 2. Comparison of DER

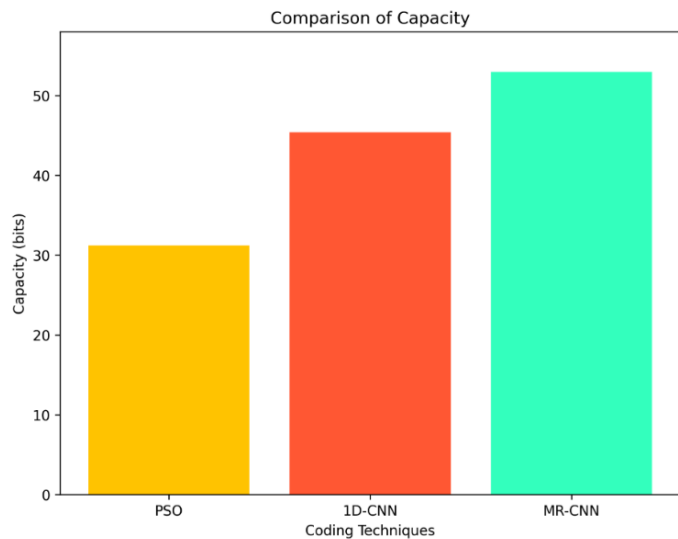


Fig. 3. Comparison of capacity

Considering an SNR of 454.78, PSO is superior to 1D-CNN (678.67) and MR-CNN (767.78) in an analysis of metrics related to performance. The BER is 232.13 for MR-CNN, 432.13 for 1D-CNN, and 567.23 for PSO. The best three models for SER are PSO (678.56), 1D-CNN (612.67), and MR-CNN (412.78). With a FER of 354.78, MR-CNN is at the bottom of the pack, next to 1D-CNN at 512.68 and PSO at 567.56. PSO emerges in third. With 31.23 bits, PSO has the highest capacity, next to 1D-CNN with 45.4 bits and MR-CNN with 53 bits. Although MR-CNN outperforms in SNR and capacity, it exhibits superior results across error rates, showing consistency in data integrity. According to these measures, 1D-CNN is in the middle. The contrast is demonstrated visually in Fig. 1 to Fig. 3. Fig. 1 indicates SNR, Fig. 2 potentially displays various error rates, and Fig. 3 exhibits distinct capacities. Overall, MR-CNN proves a higher error rate reduction than PSO, rendering it an excellent choice for tasks that are sensitive to errors, even though PSO has superior SNR and throughput.

V. CONCLUSION AND FUTURE WORK

This research highlights the importance of RFID tags without chips for automatic data capture and human identification, as they facilitate fast and secure communication.

The primary goal of this study is to improve the encoding efficiency and physical adaptability of chipless RFID tags. It is done by optimizing their resonant model. This study advances the design of chipless RFID tags by introducing an open-ended quarter-wavelength stub multi-resonator model, which provides access to real-world applications that require high-capacity data transfer. Implementing CNN for dynamic modulation and ECC improves tag performance. Both the novel AMS and ECC cooperate to make data accurate by adjusting modulation parameters in response to changes in the channel. When it comes to systems that are sensitive to errors, MR-CNN exhibits considerable potential due to its improved error rate reduction. The results of this work help to push chipless RFID forward, which is positive for various industries that use secure, high-capacity data transfer.

Further developments in chipless RFID tag design could be a focus of future studies. This may involve investigating novel resonant structures or identifying methods to optimize manufacturing for enhanced performance and scalability. The accuracy of data transfer and the validity of tags might be enhanced by investigating the possibility of integrating complex error correction coding and modulation techniques.

REFERENCES

- [1] Vena, A., Perret, E., & Tedjini, S. (2011). Chipless RFID tag using hybrid coding technique. *IEEE Transactions on Microwave Theory and Techniques*, Vol. 59, No. 12, pp. 3356-3364.
- [2] Herrojo, C., Paredes, F., Mata-Contreras, J., & Martín, F. (2019). Chipless-RFID: A review and recent developments. *Sensors*, Vol. 19, No. 15, pp. 385.
- [3] Abdulkawi, W. M., & Sheta, A. F. A. (2019). K-state resonators for high-coding-capacity chipless RFID applications. *IEEE Access*, Vol. 7, pp. 185868-185878.
- [4] Rance, O., Siragusa, R., Lemaitre-Auger, P., & Perret, E. (2016). Toward RCS magnitude level coding for chipless RFID. *IEEE Transactions on Microwave Theory and Techniques*, Vol. 64 No. 7, pp. 2315-2325.
- [5] Khaliel, M., El-Awamry, A., Megahed, A. F., & Kaiser, T. (2017). A novel design approach for co/cross-polarizing chipless RFID tags of high coding capacity. *IEEE Journal of Radio Frequency Identification*, Vol. 1, No. 2, pp. 135-143.
- [6] Vena, A., Perret, E., & Tedjini, S. (2016). *Chipless RFID based on RF encoding particle: realization, coding and reading system*.
- [7] Majidifard, S., Ahmadi, A., Sadeghi-Fathabadi, O., & Ahmadi, M. (2015). A novel phase coding method in chipless RFID systems. *AEU-International Journal of Electronics and Communications*, Vol. 69, No. 7, pp. 974-980.
- [8] Vardhan, G. S., Sivadasan, N., & Dutta, A. (2016). QR-code-based chipless RFID system for unique identification. *IEEE International Conference on RFID Technology and Applications (RFID-TA)*, pp. 35-39.
- [9] Khaliel, M. et al., (2017). Printable, high coding capacity chipless RFID tags for low-cost item tagging. *IEEE 14th International Conference on Networking, Sensing and Control*, pp. 351-355.
- [10] Tedjini, S., et al., (2013). Hold the chips: Chipless technology, an alternative technique for RFID. *IEEE Microwave Magazine*, Vol. 14, No. 5, pp. 56-65.
- [11] Abdulkawi, W. M., & Sheta, A. A. (2020). High coding capacity chipless radio frequency identification tags. *Microwave and Optical Technology Letters*, Vol. 62, No. 2, pp. 592-599.
- [12] Babaecian, F., & Karmakar, N. C. (2018). Hybrid chipless RFID tags-a pathway to EPC global standard. *IEEE Access*, Vol. 6, pp. 67415-67426.
- [13] Aliasgari, J., Forouzandeh, M., & Karmakar, N. (2020). Chipless RFID readers for frequency-coded tags: Time-domain or frequency-domain?. *IEEE Journal of Radio Frequency Identification*, Vol. 4, No. 2, pp. 146-158.

- [14] Betancourt, D., et al. (2017). Design of printed chipless-RFID tags with QR-code appearance based on genetic algorithm. *IEEE Transactions on Antennas and Propagation*, Vol. 65, No. 5, pp. 2190-2195.
- [15] Zheng, F., et al., (2018). On the coding of chipless tags. *IEEE Journal of Radio Frequency Identification*, Vol. 2, No. 4, pp. 170-184.
- [16] El-Awamry, A., Khaliel, M., Fawky, A., El-Hadidy, M., & Kaiser, T. (2015). Novel notch modulation algorithm for enhancing the chipless RFID tags coding capacity. *IEEE International Conference on RFID*, pp. 25-31.
- [17] Vena, A., Perret, E., & Tedjini, S. (2012). A compact chipless RFID tag using polarization diversity for encoding and sensing. *IEEE International Conference on RFID*, pp. 191-197.
- [18] Le, C. C., et al., (2023). Encoding Capacity Enhancement for Chipless RFID Tag Using Resonant Frequency Placement. *IEEE Access*.
- [19] Rather, N. et al. (2024). Machine learning approaches for EM signature analysis in chipless RFID technology.
- [20] Rather, N., Simorangkir, R. B., & Buckley, J. (2023). Deep learning assisted robust detection techniques for a chipless.
- [21] Sridhar Panneerselvam et al., (2024), Federated learning-based fire detection method using local MobileNet, *Scientific Reports*, vol. 14, No. 30388, pp. 1-24,
- [22] Asir Chandra Shinoo Robert Vincent and Sudhakar Sengan, (2024). Edge computing-based ensemble learning model for health care decision systems, *Sci Rep* 14, 26997.
- [23] Asir Chandra Shinoo, Robert Vincent and Sudhakar Sengan, Effective clinical decision support implementation using a multi-filter and wrapper optimisation model for Internet of Things based healthcare data. *Sci Rep* 14, 21820.
- [24] Gulista Khan et al. (2024) Energy-Efficient Routing Algorithm for Optimizing Network Performance in Underwater Data Transmission Using Gray Wolf Optimization Algorithm, *Journal of Sensors*, Vol. 2024, No. 2288527, 1-15.
- [25] Sudhakar Sengan et al. 2023, Improved LSTM-Based Anomaly Detection Model with Cybertwin Deep Learning to Detect Cutting-Edge Cybersecurity Attacks, *Human-centric Computing and Information Sciences*, Vol. 13, No. 55.
- [26] Varatharaj Myilsamy et al., (2023). State-of-Health Prediction for Li-ion Batteries for Efficient Battery Management System Using Hybrid Machine Learning Model, *Journal of Electrical Engineering & Technology*.
- [27] Indumathi Nallathambi et al. (2023). Impact of Fireworks Industry Safety Measures and Prevention Management System on Human Error Mitigation Using a Machine Learning Approach, *Sensors*, 23 (9), 4365.
- [28] Vinothini Arumugham et al. (2023) An Artificial-Intelligence-Based Renewable Energy Prediction Program for Demand-Side Management in Smart Grids, *Sustainability*, Vol. 15, No. 6, 5453.
- [29] Rasheed Abdulkader et al. (2023), Soft Computing in Smart Grid with Decentralized Generation and Renewable Energy Storage System Planning, *Energies*, Vol. 16, No. 6, 2655.
- [30] Parkavi Krishnamoorthy et al. (2023). Effective Scheduling of Multi-Load Automated Guided Vehicle in Spinning Mill: A Case Study, *IEEE Access*.
- [31] Arodh Lal Karn et al. (2023). IoT Based Smart Framework Monitoring System for Power Station, *Computers, Materials & Continua*, Vol. 74, No. 3, pp. 6019-6037.
- [32] Arul Rajagopalan et al. 2022, Oscar Danilo Montoya, Walid El-Shafai, Mostafa M. Fouda, and Moustafa H. Aly, Modernized Planning of Smart Grid Based on Distributed Power Generations and Energy Storage Systems Using Soft Computing Methods, *Energies*, Vol. 15, No. 23, 8889.
- [33] Eman S. Sabry et al. (2022), Sketch-Based Retrieval Approach Using Artificial Intelligence Algorithms for Deep Vision Feature Extraction, *Axioms*, Vol. 11, No. 12, pp. 663.
- [34] Arodh Lal Karn et al. (2022). Measuring the Determining Factors of Financial Development of Commercial Banks in Selected SAARC Countries, *Journal of Database Management*, Vol. 33, No. 1, 2022 pp. 1–21.
- [35] Prabu Selvam et al. (2022) A Transformer-Based Framework for Scene Text Recognition, *IEEE Access*, Vol. 10, pp. 100895-100910.
- [36] Arodh Lal Karn et al. (2022) Fuzzy and SVM-Based Classification Model to Classify Spectral Objects in Sloan Digital Sky, *IEEE Access*, Vol. 10, pp. 101276-101291.
- [37] Tribhuvan Kumar et al. (2022). Fuzzy Logic and Machine Learning-Enabled Recommendation System to Predict Suitable Academic Program for Students, *Mathematical Problems in Engineering*, vol. 2022, No. 5298468, pp. 1-7.
- [38] Roy Setiawan et al. (2022). IoT Based Virtual E-Learning System for Sustainable Development of Smart Cities, *Journal of Grid Computing*, Vol. 20, No. 24.
- [39] S. Priyadarsini et al. (2022), Automatic Liver Tumor Segmentation in CT Modalities Using MAT-ACM, *Computer Systems Science and Engineering*, vol. 43, no. 3, pp. 1057–1068, 2022.
- [40] S. Priyadarsini et al. (2022). Classification of Liver Tumors from Computed Tomography Using NRSVM, *Intelligent Automation & Soft Computing*, Vol. 33, No. 3, 2022, pp. 1517-1530.
- [41] Thirumoorthy Palanisamy et al. (2022) Improved Energy Based Multi-Sensor Object Detection in Wireless Sensor Networks, *Intelligent Automation & Soft Computing*, Vol. 33, No. 1, pp.227-244.
- [42] Omaira Bamasaq et al. (2022). Syed Hamid Hassan, Distance Matrix and Markov Chain Based Sensor Localization in WSN, *Computers, Materials & Continua*, Vol. 71, No. 2, pp. 4051-4068,
- [43] Sudhakar Sengan et al. (2021), Real-Time Automatic Investigation of Indian Roadway Animals by 3D Reconstruction Detection Using Deep Learning for R-3D-YOLOv3 Image Classification and Filtering, *Electronics*, Vol. 10, No. 24, 3079.
- [44] Abolfazl Mehbodniya et al. (2021). Fetal health classification from cardiocographic data using machine learning, *Expert Systems*.
- [45] Sudhakar Sengan et al. (2021). A Secure Recommendation System for Providing Context-Aware Physical Activity Classification for Users, *Security and Communication Networks*, Vol. 2021, No. 4136909, pp. 1-15.
- [46] Vasanthi Raghupathy et al. (2022). Interactive Middleware Services for Heterogeneous Systems, *Computer Systems Science and Engineering*, Vol. 41, No. 3, pp. 1241-1253.
- [47] Abolfazl Mehbodniya et al. (2022). Proportional Fairness Based Energy Efficient Routing in Wireless Sensor Network, *Computer Systems Science and Engineering*, Vol. 41, No. 3, pp. 1071-1082.
- [48] D. Stalin David et al. (2022), Enhanced Detection of Glaucoma on Ensemble Convolutional Neural Network for Clinical Informatics, *Computers, Materials & Continua*, Vol. 70, No. 2, pp. 2563-2579, .
- [49] D. Stalin David et al. (2022). Cloud Security Service for Identifying Unauthorized User Behaviour, *CMC-Computers, Materials & Continua*, Vol. 70, No. 2, pp. 2581-2600.
- [50] Ngangbam Phalguni Singh et al. 2021. Investigation on characteristics of Monte Carlo model of single electron transistor using Orthodox Theory, *Sustainable Energy Technologies and Assessments*, Vol. 48, 101601.
- [51] K. Rajakumari et al., (2022), Fuzzy Based Ant Colony Optimization Scheduling in Cloud Computing, *Computer Systems Science and Engineering*, Vol. 40, No. 2, pp. 581-592.
- [52] Arodh Lal Karn et al. (2021), An integrated approach for sustainable development of wastewater treatment and management system using IoT in smart cities, *Soft Computing*.
- [53] R. Nithya et al., (2022). Edwin Hernan Ramirez-Asis, Priya Velayutham, V. Subramaniaswamy, Sudhakar Sengan, An Optimized Fuzzy Based Ant Colony Algorithm for 5G-MANET, *Computers, Materials & Continua*, Vol. 70, No. 1, pp: 1069–1087.
- [54] Razia Sulthana Abdul Kareem et al., (2021). Multilabel land cover aerial image classification using convolutional neural networks, *Arabian Journal of Geosciences*, Vol. 14, No. 1681.
- [55] Roy Setiawan et al., Utilizing Index-Based Periodic High Utility Mining to Study Frequent Itemsets, Springer, *Arabian Journal for Science and Engineering*, 2021.
- [56] K. Muthumayil et al., (2021) A Big Data Analytical Approach for Prediction of Cancer Using Modified K-Nearest Neighbour Algorithm, *Journal of Medical Imaging and Health Informatics*, Vol. 11, No. 8, pp. 2120-2125 (6).

- [57] Keerthana Nandakumar et al. (2021) Sudhakar Sengan, Securing data in transit using data-in-transit defender architecture for cloud communication, *Soft Computing*.
- [58] Huidan Huang *et al.* (2021) Emotional intelligence for board capital on technological innovation performance of high-tech enterprises, *Aggression and Violent Behavior*, 101633
- [59] Sudhakar Sengan *et al.* (2021) Detection of false data cyber-attacks for the assessment of security in smart grid using deep learning, *Computers & Electrical Engineering*, Vol. 93, 107211.
- [60] Sudhakar Sengan *et al.*, (2021). Cost-effective and efficient 3D human model creation and re-identification application for human digital twins, *Multimedia Tools and Applications*, 2021. DOI:10.1007/s11042-021-10842-y.
- [61] Omnia Saidani Neffati *et al.*, (2021). Migrating from traditional grid to smart grid in smart cities promoted in developing country, *Sustainable Energy Technologies and Assessments*, Vol. 45.
- [62] Prabhakaran Narayanan *et al.* (2021) Novel Collision Detection and Avoidance System for Mid-vehicle Using Offset-Based Curvilinear Motion. *Wireless Personal Communication*.
- [63] Balajee Alphonse *et al.*, (2021). Modeling and multi-class classification of vibroarthrographic signals via time domain curvilinear divergence random forest, *J Ambient Intell Human Comput*.
- [64] Omnia Saidani Neffati *et al.*, (2021). An educational tool for enhanced mobile e-Learning for technical higher education using mobile devices for augmented reality, *Microprocessors and Microsystems*, Vol. 83, 104030.
- [65] Prabhakaran Narayanan *et al.*, (2021). Analysis and design of fuzzy-based manoeuvring model for mid-vehicle collision avoidance system. *J Ambient Intell Human Comput*.
- [66] Sudhakar Sengan *et al.*, (2021) Network Embedding Architecture using Laplace Regularization-Non-Negative Matrix Factorization for Virtualization, *Microprocessors and Microsystems*.
- [67] K. Sathish Kumar et al. (2020). Area Based Efficient and Flexible Demand Side Management To Reduce Power And Energy Using Evolutionary Algorithms, *Malaysian Journal of Computer Science*, 27335.
- [68] L. Arokia Jesu Prabhu *et al.*, (2020) Medical Information Retrieval Systems for e-Health Care Records using Fuzzy Based Machine Learning Model, *Microprocessors and Microsystems*, DOI:10.1016/j.micpro.2020.103344.
- [69] N. Sathesh et a., (2020). Flow-based Anomaly Intrusion Detection using Machine Learning Model with Software Defined Networking for OpenFlow Network, *Microprocessors, and Microsystems*.
- [70] Sengan Sudhakar *et al.*, (2020). A fuzzy-based high-resolution multi-view deep CNN for breast cancer diagnosis through SVM classifier on visual analysis, *Journal of Intelligent & Fuzzy Systems*, pp. 1-14.
- [71] Sengan Sudhakar et al. (2020). Images super-resolution by optimal deep AlexNet architecture for medical application: A novel DOCALN, *Journal of Intelligent & Fuzzy Systems*, pp. 1-14.
- [72] V. Vijaya Kumar *et al.* (2020). Design of peer-to-peer protocol with sensible and secure IoT communication for future internet architecture, *Microprocessors and Microsystems*, Vol. 78.
- [73] Sudhakar Sengan *et al.*, (2020). Enhancing cyber-physical systems with hybrid smart city cyber security architecture for secure public data-smart network, *Future Generation Computer Systems*.
- [74] Ganesh Kumar, K and Sudhakar Sengan (2020) Improved Network Traffic by Attacking Denial of Service to Protect resources using Z-Test Based 4-Tier Geomark Traceback (Z4TGT), *Wireless Personal Communications*.
- [75] S. Sudhakar *et al.* (2020). Unmanned Aerial Vehicle (UAV) based Forest Fire Detection and monitoring for reducing false alarms in forest fires, *Computer Communications* 149, pp. 1–16.
- [76] Sudhakar Sengan and Chenthur Pandian S, (2016), Hybrid Cluster-based Geographical Routing Protocol to Mitigate Malicious Nodes in Mobile Ad Hoc Network, *International Journal of Ad Hoc and Ubiquitous Computing*, Vol. 21, No. 4, pp. 224-236.